DATA REPOSITORY

1. Possible submarine volcanism near Nicobar Islands.

On January 24 2005 an earthquake swarm began east of the Nicobar Islands. Until January 30 2005 about hundred Mw≥5 shallow earthquakes (depth < 15 km) were recorded within a 50 km distance to latitude 7.98 longitude 94.13. The seafloor is at 1800 m depth. A likely explanation for the seismic swarm is a submarine volcanic eruption or unrest at a submarine volcano although no unusual degassing was reported at the sea surface.

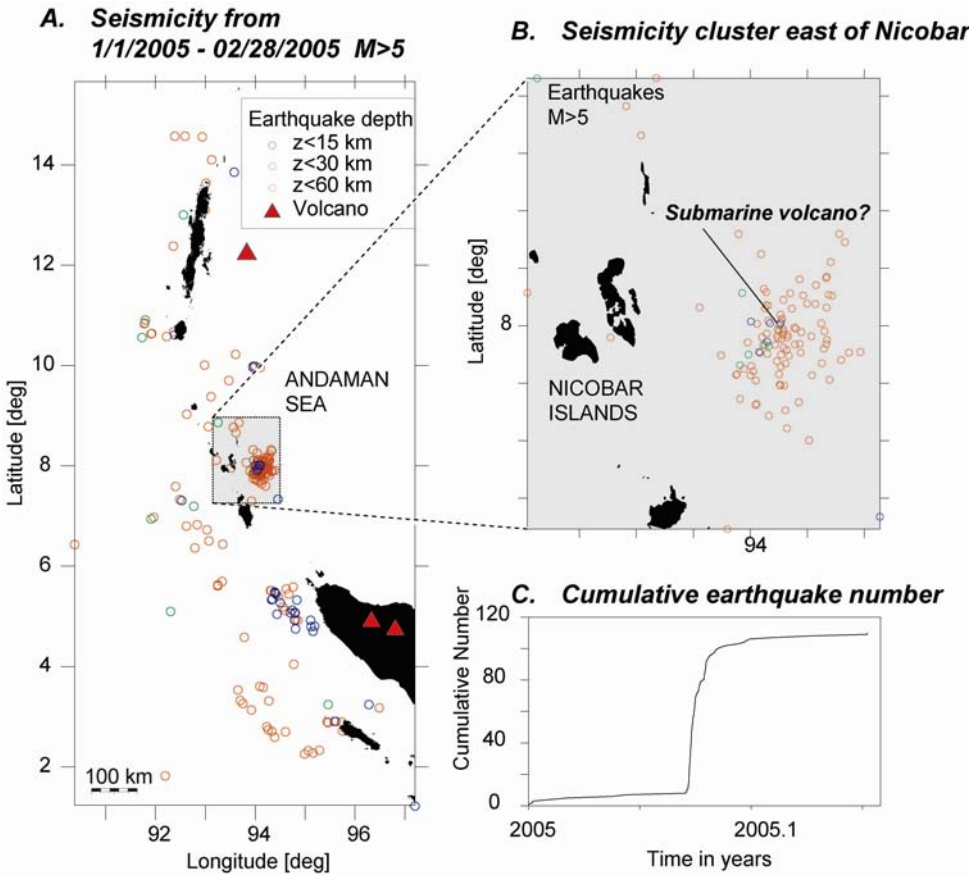

Figure DR1. A. Earthquakes with magnitude Mw≥5 from January - February 2005 near the rupture zone of the Sumatra-Andaman earthquake. B. Zoom-in on the area of a seismic swarm east of the Nicobar Islands. C. Cumulative number of Mw>5 earthquakes located within B (Data from the Advanced National Seismic System (ANSS) online catalogue).

2. Modelling

The geometry of the model subduction zones is summarized in Table DR1, and shown in Figure DR2.

	Subduction parameters					Earthquake parameters					
	Upper plate	Lower plate [age in Ma]	Mean conv. rate [mm]	Depth of slab below volcanoes	Distance of volcanoes to trench	Date [mm/dd/yyyy]	Epicenter [lat/long, depth]	M	Rupture length [km]	Rupture plane dip [°]	Rupture width [km]
Kamchatka	Eurasia	Pacific [90]	76	95	200-250	11/04/1952	159.5˚E 52.75˚N	9.0	600-700	10-15	100
Chile	South America	Nazca [34]	67-78	110-125	260-220	05/22/1960	72.34˚W 38.5˚S	9.5	900	20-25	150
Alaska	North America	Pacific [46]	56	85	150-450	03/28/1964	147.73˚W 61.04˚N	9.2	800	6-12	300
Sumatra	Indo-Austral	Sunda [50]	47	115	220-300	12/26/1904	94.35˚E 4.13˚N	9.3	1300	11-35	160

Table DR1. Subduction and earthquake parameters for the 4 largest megathrust earthquakes with simplified convergence rates (DeMets et al., 1994) and slab geometries (England et al., 2004).

We base the models on published fault slip distributions of the earthquakes.

For the M9.0 1952 Kamchatka earthquake our model consists of 12 subfaults of 100 x 100 km area (Figure DR2 A), a constant dip of 13°, strike of 214°, slip direction N76°W and slip rates of up to 11.4 m (Johnson and Satake, 1999).

For the M9.5 1960 Chile earthquake we sampled the available variable slip model (Barrientos and Ward, 1990) along rectangular dislocation planes 100 km long by 50 km wide (Figure DR2 B). The rupture plane has a length of 1200 km, with a constant dip of 20°, strike of 7°N, rake of 105°, and slip rates of as much as 40 m at two asperities (Barrientos and Ward, 1990).

For the M9.2 Alaska earthquake we use 28 rectangular fault patches (~50 x 50 km each) in the Kodiak Island region, oriented 218°N, with a dip between 8° and 9°, and 39 fault patches (~40 x 50 km near the trench, 64 by 50 km inland) in the Prince William Sound

region (Holdahl and Sauber, 1994), orientation from 218°N in the west to 270°N in the east (Figure DR2 C). The slip maxima are near Montague Island (30 m), and near Kayak Island (14 m). A further dislocation plane dipping 30°NW according to the active Patton Bay fault was also considered in the model (Holdahl and Sauber, 1994).

For the Sumatra-Andaman rupture models we use two published slip models, one to simulate the M9.3 2004 earthquake (Banerjee et al., 2005) and another one to simulate the M8.7 2005 earthquake (Yagi, 2005). The 2004 rupture geometry is simulated by 3 main fault segments, each consisting of several rectangular fault planes, striking from 322° in the south to 24° in the north, with a shallow part from 0 to 30 km depth and dips between 11° and 18°, and a deeper part from 30 to 50 depth with dip angles of 35°. The 2005 rupture geometry is simulated by a single rectangular fault plane 310 x 170 km, strike 329°, and dip 15° (Figure DR2 D). The patches have a slip direction that is trench perpendicular, rake 90°, in the south, and becomes highly oblique 104° in the north, with slip rates of up to 9.2 m. Further details of the herein used slip models can be found in (Banerjee et al., 2005; Barrientos and Ward, 1990; Holdahl and Sauber, 1994; Johnson and Satake, 1999; Yagi, 2005).

In order to calculate volumetric deformation at the line of active volcanoes, we define vertical observation planes that follow the coordinates of the historically active volcanoes for a length of 3000 km, with a depth from 0 to 50 km. Grid spacing is 2 km, where the axial components of strain exx, eyy, and ezz are computed (see Figure DR2).

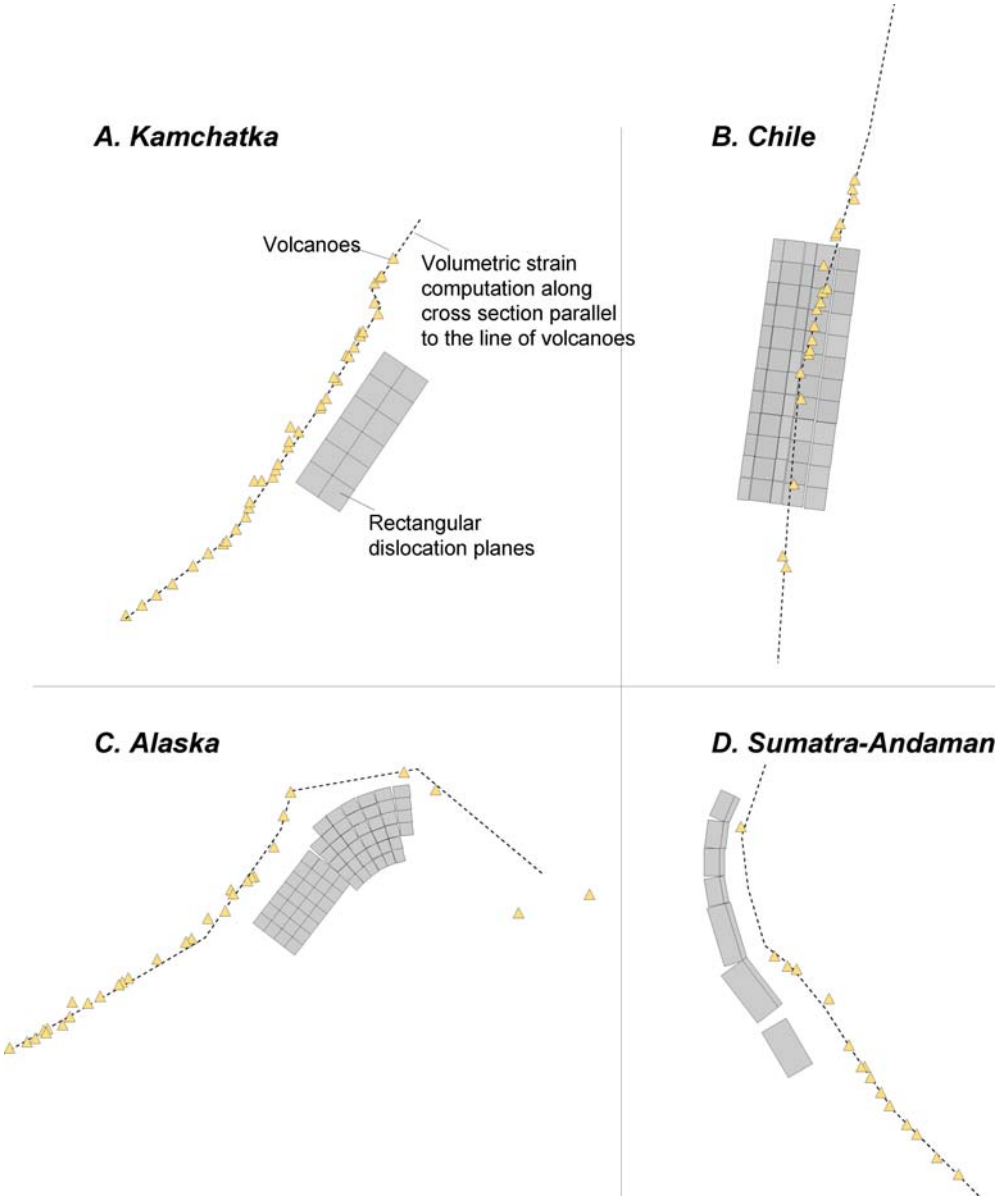

Figure DR2. Subduction geometries considered in the four studied model calculations. Coseismic earthquake dislocation is approximated by 12 rectangular fault planes for the Kamchatka earthquake, 60 fault planes for the Chile earthquake, 68 fault planes for the Alaska earthquake and 13 fault planes for the Sumatra-Andaman earthquake

3. Statistical significance

The results of the statistical analysis depend on a homogeneous dataset. Irregular reporting and increased awareness after large earthquake pose a problem. For example, there were reports about volcanism in the Banda Aceh area after the December 2004 Sumatra earthquake, which later turned out to be false alarms. We attempt to circumvent this problem by considering only explicitly confirmed eruptions. Unconfirmed eruptions and eruptions for which the exact date (year and month) and locality (volcano) is not known are removed from our catalogue. A comparison of the average eruption rate versus the post-earthquake average eruption rate is given in the Table DR2 below.

Earthquake date [mm/dd/yyyy]	Volcano types	50 yrs before the earthquake		Post-earthquake eruptions	AER [eruptions/yr]	PER [eruptions/yr]	PER/ AER
		Erupting volcanoes	No. of eruptions				
All four arcs combined	1	0	0	5	0	1.7	Nd
	2	33	63	10	1.3	3.3	2.7
	3	8	67	6	1.3	2.0	1.5
Kamchatka,11/04/1952	1 and 2	17	29	5	0.6	1.7	2.9
	3	3	28	3	0.6	1.0	1.8
Chile, 05/22/1960	1 and 2	10	22	6	0.4	2.0	4.6
	3	1	10	1	0.2	0.3	1.7
Alaska, 03/28/1964	1 and 2	2	3	2	0.1	0.7	8.3
	3	3	19	1	0.4	0.3	0.8
Sumatra, 12/26/2004	1 and 2	4	9	2	0.2	0.7	3.7
	3	1	10	0	0.2	0.0	0.0

Table DR2. Average eruption rate (AER) for the fifty year period before the earthquakes and the post-earthquake eruption rate (PER) for a 3 year period following the earthquakes for rarely (type 1 and 2) and for more frequently erupting volcanoes (type 3, see text for definitions). Note that at some volcanoes repeated eruptions occurred, thus the number of eruptions listed here may differ from the number of volcanoes listed in the main text. The Sumatra statistics does not consider the submarine seismic swarm as an eruption because of the uncertainty of its volcanic origin.

To more rigorously test whether the increases in eruption rate are statistically significant and to avoid any subjective data analysis and filtering, we compare the rate of all eruptions during a running three years time window with the long term average using a β-statistic. The method is a standard used in statistical seismology (Matthews and Reasenberg, 1988)32. We first calculate $\beta = (No - Ne) / (Ne(1-p))1/2$, where Ne and No are the expected and observed numbers of events in the subinterval, and p is the ratio of the duration of the anomalous period to the duration of the entire sample. In order to determine the time of eruption rate changes we then compute this β-statistics repeatedly constructing a function, LTA(t) (Long Term Average function after Habermann, 1988, 1991), and comparing the value β within a window βwl to the background rate βall. We used a 3 year window which is moved from 1900 to 2005 in 1-year steps. The significance level is determined based on a random simulation compared to a uniform Poissonian time series, and considered significant if within 1% interval. We find a total of 12 significant rate increases between 1900 and 2005, six of which coincide with large earthquakes. The megathrust earthquakes in Kamchatka, Chile and Alaska all correlate to significant eruption rate increases. Rate increases also correlate with a 1923 M8.5 earthquake in Kamchatka, a 1906 M8.6 earthquake in Chile, and 1915 M8.1 and 1969 M8.2 earthquakes in Sumatra.

Using a time window of 3 years the β-test shows since 1900 a total of 11 statistically significant rate increases in Kamchatka, Chile and Alaska, 6 of which correlate with large earthquakes (Figure DR3). In Kamchatka since the early 1920s (the installation of the Kamchatka volcanological station) the cumulative number of eruptions is relatively constant (Figure DR3). Significant rate increases in 1923 and 1956 correlate with a 1923 M8.5 earthquake and with the 1952 M9.0 event. In Chile significant rate increases in 1906 and 1959 correlate with the 1906 M8.6 and 1960 M9.5 earthquake events, respectively. The rate increase that correlates with the 1960 Chile earthquake in fact commences shortly before the

earthquake, which may be related to preslip at the seismogenic fault that occurs within the months to years prior to large earthquakes - similar as recently suggested for the Alaska and Cascadia subduction zones in the northwestern USA (Bourgeois, 2006). However, no further geophysical or geological data supports this hypothesis for the Andes yet. A further rate increase in 1930 is less significant but correlates with the 1930 M8.3 earthquake. In Alaska the increase of eruption rate in the 20th century can be attributed to improved reporting. The statistically significant rate increase in 1964 correlates with the 1964 M9.2 event. In Sumatra the dataset is biased by irregular reporting, strongly increasing since the 1980ies, where two rate increases correlate to earthquakes, one in 1916 correlates with the 1915 M8.1 earthquake, and one in 1966 may be related to the 1969 M8.2 earthquake. Significant rate increases that do not correlate with earthquakes occurred in 1984 in Kamchatka, 1994 in Chile, and 1974 and 1985 in Alaska. In Sumatra-Andaman there were not enough eruptions for reliable rate analysis. There was no eruption between 1920 and 1963. Therefore we do not consider the 1999 rate increase as significant.

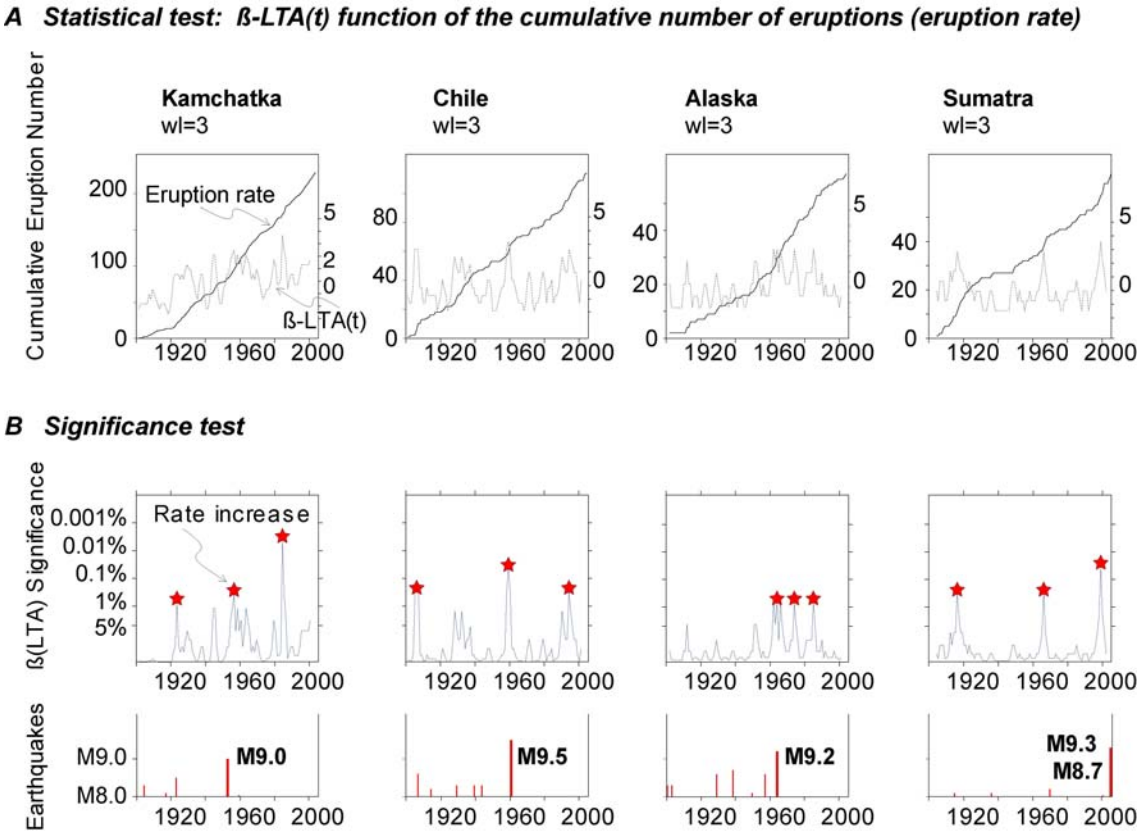

Figure DR3. Time series and statistical test of volcanic eruptions in the four arcs. (A) Eruption rate, given by the cumulative number of eruptions from 1900 – 2005. The beta-statistical analysis (dashed line) shows rate changes shown by peaks and lows. (B) The test of the statistical significance of the rate changes is marked by a star if above 99% level. Statistically significant rate increases isochronous to the herein studied megathrust-earthquakes occurred in Kamchatka (1953), Chile (1961), and Alaska (1963). The rate increase in following the Sumatra-Andaman earthquake is not significant yet.

References cited in electronic data repository

Banerjee, P., Pollitz, F.F., and Burgmann, R., 2005, Geophysics: The size and duration of the Sumatra-Andaman earthquake from far-field static offsets: Science, v. 308, p. 1769-1772.

Barrientos, S.E., and Ward, S.N., 1990, The 1960 Chile earthquake; inversion for slip distribution from surface deformation: Geophysical Journal International, v. 103, p. 589-598.

Bourgeois, J., 2006, A movement in four parts?: Nature, v. 440, p. 430-431.

DeMets, C., Gordon, R.G., Argus, D.F., and Stein, S., 1994, Effect of recent revisions to the geomagnetic reversal time scale on estimates of current plate motions: Geophysical Research Letters, v. 21, p. 2191-2194.

England, P., Engdahl, R., and Thatcher, W., 2004, Systematic variation in the depths of slabs beneath arc volcanoes: Geophysical Journal International, v. 156, p. 377-408.

Holdahl, S.R., and Sauber, J., 1994, Coseismic slip in the 1964 Prince William Sound earthquake: a new geodetic inversion: Pure and Applied Geophysics, v. 142, p. 55-82.

Johnson, J.M., and Satake, K., 1999, Asperity distribution of the 1952 great Kamchatka earthquake and its relation to future earthquake potential in Kamchatka: Pure and Applied Geophysics, v. 154, p. 541-553.

Yagi, Y., 2005, http://iisee.kenken.go.jp/staff/yagi/eq/Sumatra2004/Sumatra2004.html.